Comparative Durability of GFRP bars in Concrete and in Simulated Concrete Environment

Abstract
Many studies suggest that the durability of glass fiber reinforced polymer (GFRP) bars in simulated concrete pore solution is very different than an actual concrete environment. This study therefore provides a comparative evaluation on the durability of GFRP bars in concrete and in simulated concrete environment through the investigation of their interlaminar shear strength. It focuses on the evaluation of the physical, mechanical and micro-structural properties of GFRP bars under high moisture, saltwater and alkali environments. Bare GFRP bars and cement-embedded GFRP bars were immersed in solutions at different temperatures (23^{o}C, 60^{o}C and 80^{o}C) and exposure times (28 days, 56 days and 112 days). The results showed that the percentage water uptake and the apparent diffusivity of the GFRP bars were strongly dependent on the type of immersion solution and temperature. Direct immersion in solution were found to more severely deteriorate the interlaminar shear strength of bare GFRP bars than cement embedded bars. Moreover, alkaline solution was more aggressive to GFRP bars than tap water and saline solution affecting its fiber and matrix interface, and chemical structure for bars exposed after 112 days. As a result of this study, master curves and time shift factor were developed to correlate the interlaminar shear strength retention from the accelerated aging test to the service life of GFRP bars in actual concrete environment.

Keywords: GFRP reinforcing bars; interlaminar shear strength; cement embedded bars; comparative durability; alkaline solution; time shift factor.

Introduction

Glass fibre-reinforced polymer (GFRP) bars have emerged as a promising and cost-effective replacement for steel to increase the useful life of reinforced concrete structures exposed in severely aggressive environments. Research and development related to this high tensile strength, lightweight, non-corrosive, non-magnetic, and non-electrical conductive reinforcing material has been carried out extensively in the US, Canada, Europe, and Japan (Benmokrane et al. 2017) leading to the many successful field applications of GFRP reinforced concrete structures including highway bridges and barriers, pavements and parking garages, storage facilities for chemical and wastewater treatment plants, magnetic-resonance-imaging facilities, detector loops in railway lines, and temporary structures such as soft-eyes in underground excavations and tunnelling works. This composite reinforcing material is now also being increasingly utilised in Australia as a main reinforcement in concrete structures that operate near coastline and in aggressive soils (Maranan et al. 2016, Manalo et al. 2014, Ferdous et al. 2015). As internal reinforcement, GFRP bars are continuously subjected to alkaline environment due to its surrounding concrete and other environmental conditions that may affect their physical, mechanical and long-term durability properties. Many researchers have suggested that the high alkalinity of concrete pore-solution is an aggressive environment for the GFRP bars, which could cause damages at the glass fibers and/or deteriorate the fiber-resin interface (Chin et al. 2001, Tannous and Saadatmanesh 1999, Karbhari and Zhang 2003, Belarbi and Wang 2012, Benmokrane et al. 2017a). Similarly, infrastructure systems are exposed to external agents during their service life including high moisture, alkalinity and

saline environment which can damage the properties of GFRP bars (Nkurunziza et al. 2005). Due to the limited understanding on the durability of GFRP bars, Ceroni et al. (2006) and Karbhari and Zhang (2003) indicated that designers apply very conservative factors of safety to account for the unquantified, detrimental effects which vanishes the high-strength performance of this reinforcing material. Thus, Micelli and Nanni (2004) and Gooranorimi and Nanni (2017) highlighted the importance of understanding the long-term and durability performance of GFRP bars in different aggressive environmental conditions as these are critical to their widespread acceptance in civil infrastructure.

In recent years, significant effort was exerted to study the effects of highly aggressive environment on the durability of GFRP bars. In most cases, the durability of this reinforcing material is determined based on the changes in bar mechanical properties following accelerated testing and evaluation programs using bare GFRP bars. Kim et al. (2008) directly exposed GFRP bars in different solutions at room and elevated temperature to accelerate degradation, and found that alkaline solution can reduce the tensile strength of E-glass/vinyl-ester FRP bars by almost 60% after 132 days. Based on the model presented by Davalos et al. (2011), GFRP bars made of E-glass and vinyl-ester resin can retain only 38% of their tensile strength after 50-year exposure in saturated and loaded concrete at 10ºC. The results from most of these durability studies showed that GFRP bars experienced significant loss in mechanical properties and impossible to fully utilise their superior properties. However, Almusallam et al. (2012) highlighted that the accelerated laboratory experiments were too harsh compared to the real field conditions. From the results of works conducted by Robert et al. (2009), the GFRP bars embedded in moist concrete and exposed to tap water at elevated temperature can retain up to 90% of its tensile strength after 240 days of exposure. Moreover, in-field durability test indicated that there was no degradation of the GFRP bars in the concrete structures. Mufti et al. (2007) found no degradation of the GFRP bars in five concrete bridge structures across Canada after exposure to natural environmental conditions for 5 to 8 years. Gooranorimi and Nanni (2017) further validated the long-term durability of GFRP bars extracted from the concrete deck of the Sierra de la Cruz Creek Bridge in Texas, USA after 15 years of service. More recently, Benmokrane et al. (2018) reported no significant changes in the physico-chemical properties and microstructure of GFRP bars extracted from a concrete bridge barrier in the Val-Alain Bridge in Canada after 11 years of service exposure to wet-dry cycles, freeze thaw cycles, and de-icing salts. Mufti et al. (2007) pointed out that the durability of GFRP bars in actual concrete structures is very different from the results of the durability test from immersing the bars in alkaline solution in the accelerated laboratory test as the concrete itself is protecting the GFRP bars from direct exposure to various environmental conditions. Thus, a more realistic and simplistic study should be conducted to have a better understanding on the durability of GFRP bars in concrete environment. Moreover, prediction of the service-life and long-term performance of GFRP bars under different environmental factors is of immense importance to the further use of these non-corrosive reinforcing materials.

The results of the previously mentioned studies clearly indicate that the measured durability from accelerated test using bare GFRP bars subjected to simulated concrete pore solution is different from the long-term performance of bars in an actual concrete environment. D'Antino et al. (2018) in fact highlighted that the results from environmental aging of GFRP bars by different research groups showed in many cases contradictory results. Most of these studies are conducted by either characterising the tensile test properties of GFRP bars, flexural

investigation of concrete beams reinforced with GFRP bars subjected to accelerated aging test, or extraction of GFRP bars from actual concrete structures for in-field service evaluation. These investigations require significant amount of resources and time limiting the test parameters and obtained data to evaluate the durability of GFRP bars. Similarly, most durability investigations focusing on tensile strength tests measured very little change because this property is mostly defined by the mechanical properties of the fibers (Aiello et al. 2006, Ashrafi et al. 2018). Ceroni et al. (2006) and Park et al. (2008) highlighted that the accelerated aging involves exposure to moisture and elevated temperature which affects more the resin than fiber properties. Adams (2018) indicated that the short beam shear test is one of the most important type of mechanical test for composites and an excellent choice for comparative testing. This is due to the simplicity of the test method but measures the integrity of the interior of the bars specially the fibre-to-matrix adhesion. Thus, evaluation of interface property of GFRP bars using short-beam shear test can give a straightforward and reliable indication of the resistance of the fiber–matrix interface after exposure to aggressive environments.

Karbhari and Zhang (2003) suggested that glass fibers and vinylester resin systems are preferred in civil infrastructure due to considerations of cost and ease of processing. Tannous and Saadatmanesh (1999) reported that vinylester-based GFRP bars adds high protection to fibers and provides high resistance against chemical attacks. Moreover, Benmokrane et al. (2017a, 2017b) found that the vinylester-based GFRP bars can retain almost all its original tensile strength and stiffness properties even after long-term exposure to alkaline solution. Based on the short-term test results of concrete beams immersed in tap water inside temperature-controlled tanks, Davalos et al. (2011) found that the dominant degradation mechanism for GFRP bars in concrete was the deterioration of fiber/matrix interface. Wang et al. (2017) also indicated that the fibre resin interface is more generally easily destroyed by the aggressive solution, and it is commonly believed to be the weakest location in composite materials. Thus, Micelli and Nanni (2004) suggested that the short beam shear test can be considered a good representative in evaluating the fiber-resin interface of GFRP bars and the results may then furnish indication on possible effects on the longitudinal properties. This is due to the interlaminar shear strength (ILSS) of GFRP bars is primarily related to the resin properties and governed by the fiber-matrix interface (Benmokrane et al., 2017b). Furthermore, Benmokrane et al. (2017a) suggested that the fibre-resin interface as one of the important issues in the manufacturing of GFRP bars. As a result, this bar property was added to the recently approved CSA S807 (2019) as a new test requirement for quality assurance testing. Therefore, the variation of the interlaminar shear strength can be a good indicator of deterioration in the GFRP bars (Ceroni et al. 2006) and provide a measure of resin damage caused by the penetration of fluids, which is happening during the aging of the bars (Park et al. 2008). Despite its simplicity, durability investigation of the GFRP bars using ILSS is limited, and no work explored ILSS to evaluate the durability of GFRP bars in accelerated aging conditions and exposed to simulated concrete environment.

The current study provides a comparative evaluation on the durability of GFRP bars in concrete and in simulated concrete environment through the investigation of their interlaminar shear strength. It focuses on the evaluation of the physical, mechanical and micro-structural properties of GFRP bars under high moisture, saltwater and alkali environments. These types of environments are selected as they are considered environmental problems in reinforced concrete elements (Ceroni et al. 2006). The results from this study provide a better

understanding on the durability and long-term performance of GFRP bars for their safe design and application as internal reinforcement in concrete structures. It also provides a prediction of the service life of GFRP bars in an actual concrete environment based on the temperature time shift factor determined from accelerated aging tests.

Experimental Program

Materials

Sand-coated high modulus (HM) GFRP bars with a nominal diameter (d_b) of 9.53 mm were used in the study. The bars were manufactured using ECR-glass fibres in a modified vinyl ester resin in a pultrusion process. This type of bars was considered as they are the most commonly used reinforcement for concrete structures given their relatively low cost and high performance (Benmokrane et al. 2017b). The glass fibre content by weight of GFRP bars, determined in accordance with ISO 1172:1996(E) was 84.05%. The physical and mechanical properties of these bars determined following the appropriate CSA and ASTM test standards are reported in Table 1.

Table 1. Summary of the test methods and number of specimens

Properties	Test Method	No. of Samples	Average	Standard deviation
Physical properties				
Cross-sectional area (mm^2)	CSA-S806, Annex A (2012)	9	83.8	1.9
Fiber content by weight (%)	ASTM D3171-15 (2015)	9	80.9	0.2
Transverse CTE ($x10^{-6}$/°C)	ASTM E1131-08 (2014)	9	20.7	2.3
Void content (%)	ASTM D5117-09 (2009)	9	0	0
Water absorption at 24 hrs (%)	ASTM D570-98 (2010)	15	0.15	0.01
Water absorption at saturation (%)	ASTM D570-98 (2010)	15	0.19	0.01
Cure ratio (%)	ASTM E 1356-08 (2014)	15	100	0
T_g (°C)	ASTM E 1356-08 (2014)	15	125.8	1.3
Mechanical properties				
Flexural strength, f_u (MPa)	ASTM D4476/D4476M-14 (2014)	6	1623.7	58.2
Interlaminar shear strength, S_u (MPa)	ASTM D4475-02 (2016)	6	54.7	1.1
Tensile strength, f_t (MPa)	ASTM D7205/D7205M-06 (2011)	6	1315.3	31.1
Tensile modulus, E (GPa)			62.5	0.4

Tensile strain, *e*	2.3	0.1

Test specimens

A total of 324 specimens were prepared, conditioned and tested. The bars were divided into two series: (1) GFRP bars and (2) the cement-embedded GFRP bars as shown in Figure 1. The test specimens were cut into 40 mm length (approximately four times bar diameter, $4d_b$) from the GFRP bars manufactured from the same production lot. The cement-embedded GFRP bars (Figure 1b) were placed centrally into a 60 mm long PVC pipe filled with cement paste of 25 mm diameter cylindrical shape providing a cover of 7.5 mm around the bar and 10 mm on both ends. The GFRP bars embedded in cement are prepared to simulate the environmental conditions of reinforcements inside concrete structures. However, the thickness of the cement cover was kept to a minimum for easy removal of the bars after conditioning. The cement paste has a water-to-cement ratio of 0.45. Six (6) replicates were prepared for each specimen type as summarized in Table 1. The pH of the hardened cement paste was 12.8 as measured according to ASTM D4972 (2013).

a. GFRP bars b. Cement-embedded GFRP bars

Figure 1: Specimen types

Table 1 - Specimen details.

Tap Water		Exposure time, days						Subtotal	Total
		28		56		112			
		Bar Only	Bar in Cement	Bar Only	Bar in Cement	Bar Only	Bar in Cement		
Temp, °C	RT	6	6	6	6	6	6	36	108
	60	6	6	6	6	6	6	36	
	80	6	6	6	6	6	6	36	
Alkaline Solution		Exposure time, days						Subtotal	Total
		28		56		112			
		Bar Only	Bar in Cement	Bar Only	Bar in Cement	Bar Only	Bar in Cement		
	RT	6	6	6	6	6	6	36	108

Temp, °C	60	6	6	6	6	6	6	36	
	80	6	6	6	6	6	6	36	
Saline Solution		Exposure time, days						Subtotal	Total
		28		56		112			
		Bar Only	Bar in Cement	Bar Only	Bar in Cement	Bar Only	Bar in Cement		
Temp, °C	RT	6	6	6	6	6	6	36	108
	60	6	6	6	6	6	6	36	
	80	6	6	6	6	6	6	36	

Conditioning

The conditioning of the specimens was done by immersing the GFRP bars and cement-embedded GFRP bars in three different types of solutions, i.e. tap water (TW), saline solution (SS) and alkaline solution (AS) for 28 days, 56 days, and 112 days (672 hours, 1344 hours and 2688 hours, respectively) under three different temperatures (23°C, 60°C, and 80°C) as shown in Figure 2. These conditioning temperatures were selected as they are well below the glass transition temperature of the GFRP bars of 125.8°C as reported in Table 1. Bank et al. (2003) suggested these levels of temperature will accelerate the degradation effect of aging but ensure that the GFRP bars will not be subjected to a change of degradation mechanism. The tap water simulates high moisture condition while the saline solution was prepared in accordance with ASTM D 1141-98 (2013) using 3.5% NaCl by weight solution to match the salinity of saltwater in a marine environment. On the other hand, the alkaline solution had a pH of 12.7 to simulate the concrete environment and prepared in accordance with ASTM D7705 (2012). During the conditioning, the glass containers were constantly checked and refilled as needed to make sure that the specimens were completely submerged and covered to minimise evaporation of the liquid solution. The conditioning elevated temperatures of 60°C and 80°C were achieved by placing the glass containers inside a programmable oven.

Figure 2: Conditioning of GFRP bars

Moisture Uptake

The percentage moisture uptake of the conditioned GFRP bars (only those samples which are not embedded in cement) were measured periodically following ASTM D570 (2010). The samples were weighed to determine the initial mass (m_0) prior to conditioning. After immersion for each exposure duration, the specimen was removed from the solution, quickly washed with tap water, dried using tissue paper, and then weighed immediately (m_{1B}). Lastly, the specimen was post-conditioned, and then reweighed (m_{1A}). The percentage moisture uptake was expressed as the ratio between the weight of the water penetrated through the bars (*weight of wet specimen – weight of dry specimen*) and the weight of the dry bars, and was calculated using Equation 1:

$$Mass\ gain\,(\%) = \frac{m_{1A} - m_0}{m_0} \times 100 \qquad \text{Equation 1}$$

Short-Beam Shear Test

The long-term performance of the GFRP bars was evaluated through investigation of their interlaminar shear strength (ILSS) in accordance with ASTM D4475-02 (2016). For cement-embedded GFRP bars, the bars were carefully extracted to avoid damage using a small hammer and a flat head. It is important to note that there was no crack in the cement cover after conditioning indicating that there was no expansion in the bars and the solution did not penetrate through cracks. Short-beam test of GFRP bars with a clear span of $3d_b$ and overhanging length of $0.5d_b$ was performed. Micelli and Nanni (2004) indicated that this span will avoid flexural effects that could change the desired shear failure mode of the bars. Six samples from each group was tested to examine the inter-laminar shear strength of the conditioned and unconditioned GFRP bars. The inter-laminar shear testing was performed using MTS 100kN testing machine with a displacement-control rate of 1.3 mm/min. The actual test set-up is shown in Figure 3a. The inter-laminar shear strength, S_u, was calculated as: $S_u = 0.849P/d^2$, where P is the shear failure load (N), and d is the bar diameter (mm). The average and standard deviation of the ILSS for all the tested specimens are presented in Table 4.

The specimens was designated as based on the cement-embedded (CE) or not, followed by the type of conditioning environment (TW for tap water, SS for saline solution, and AS for alkaline solution), followed by the level of temperature (RT for room temperature or 23°C, 60 for 60°C, and 80 for 80°C), and finally the exposure duration (28, 56, and 112 days). For example, specimen CE-TW-60-112 represents the cement embedded GFRP bars conditioned in tap water at a temperature of 60°C for 112 days.

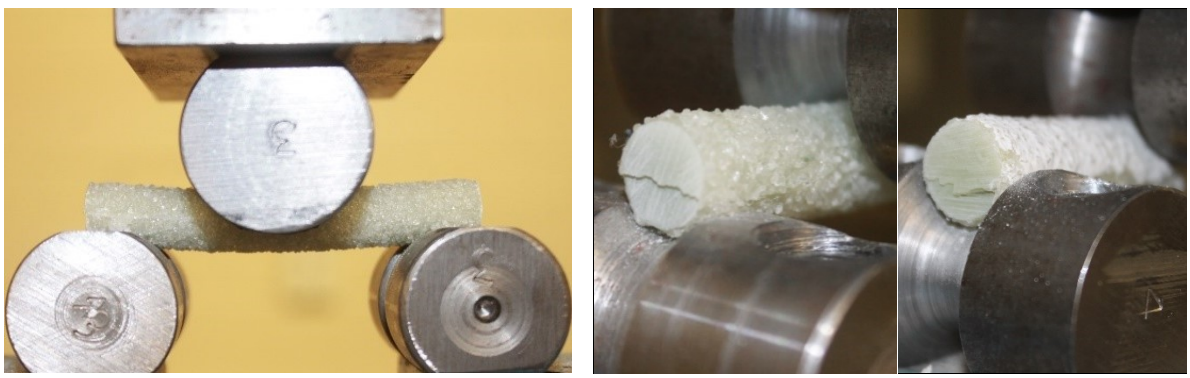

a. Test set-up b. Failure of control and conditioned bars

Figure 3: Short-Beam Shear Test

Results and Discussion

Moisture Uptake

The moisture uptake is an important factor that could significantly affect the mechanical and durability properties of GFRP bars (Benmokrane et al. 2001). Micelli and Nanni (2004) indicated that there is a strong evidence that the rate of degradation of GFRP bars exposed to fluid environment is related to the rate of sorption of the fluid. GFRP bars embedded in reinforced concrete elements can absorb moisture and water, which penetrate through the resin affecting the fiber-resin interface (Bradley and Grant 1994, Kawagoe et al. 2001). Moreover, the volume expansion of the water at low temperature causes degradation in the polymeric resin, thus, reduction in shear strengths of GFRP bars (Robert and Benmokrane 2010).

In this study, the percentage moisture uptake at different conditioning times is used to obtain quantitative information on the diffusion properties of GFRP bars in different solutions. Figure 4 shows the plot of the moisture uptake at saturation of bare GFRP bars conditioned in tap water (TW), alkaline solution (AS), and saline solution (SS) and in different temperatures (23°C, 60°C, and 80°C) against the square root of the exposure time in seconds. On the other hand, Table 2 summarises the peak moisture uptake of the GFRP bars (M_m) and the apparent diffusivity (D) in the different solution and conditioning temperature as calculated using the Fick's equation (Equation 2) for a bar-shaped specimen presented by Aiello et al. (2006):

$$D = \pi\left(\frac{d}{4.M_m}\right)^2\left(\frac{M_2-M_1}{\sqrt{t_2}-\sqrt{t_1}}\right)^2 \qquad \text{Equation 2}$$

where d is the nominal diameter of the bar, M_1 and M_2 are the moisture contents at times t_1 and t_2, respectively. Both at times t_1 and t_2, respectively. Both t_1 and t_2 are taken at times where the change in moisture uptake is relatively linearly varying with the square root of time as suggested by Karbhari and Zhang (2003).

There is obvious amount of scatter in the measured percentage moisture uptake primarily due to the relatively small mass change. In general, the moisture uptake process of GFRP bars followed the Fick's Second Law of Diffusion. The moisture uptake increased linearly in the first 28 days ($s^{1/2}$ of around 1500) and tend to stabilise after that with the increasing square root of exposure time due to the bars already reached saturation. This two-stage moisture uptake is a typical behaviour of high volume fraction unidirectional composites as also suggested by Karbhari and Xian (2009). Of particular note is the difference in percentage moisture uptake of the GFRP bars depending on the type of solution and temperature, with the percentage moisture uptake higher for higher temperature exposure indicating that temperature has a direct effect on the water absorption. As with the percentage moisture uptake, apparent diffusivity values also increase with the temperature. For similar degree of temperature exposure, the GFRP bars conditioned in the alkaline solution has the highest moisture uptake (0.16%-0.22%) as shown in Fig. 4c followed by the bars conditioned in tap water (0.14%-0.18%) and saline solution (0.12%-0.15%) as shown in Figs. 4a and 4b, respectively. The high moisture uptake in AS is due to the free OH-ions in the solution which can break the Si-O-Si structures and promote diffusion of more water inside the bar as found by Chen et al. (2007). On the other hand, Bank et al. (2003) indicated that the higher moisture uptake of composites in water than in saline solution can be attributed to the larger size of salt ions compared to that of water. Overall, it is good to note that the moisture uptake of the bars is very low and is similar to that of the percentage absorption of the straight GFRP bars samples (0.14%) measured by

Benmokrane et al. (2018). Moreover, the measured apparent diffusivity which ranges from 0.71 x 10^{-7} mm^2/s compares well with the values reported by Karbhari et al. (2002) for E-glass/vinylester composites exposed to concrete based alkali solutions. The low moisture uptake and apparent diffusivity values were also due to the less hydrophilic properties of the vinylester resin as it contain less polar ester moieties as found by Chin et al. (2001). This behaviour also suggests that the moisture was absorbed only through the resin rich surface of the GFRP bars as suggested by Mouzakis et al. (2008). The effect of this absorbed solution to the fiber-matrix interface was evaluated through the interlaminar shear strength test and discussed in the next section.

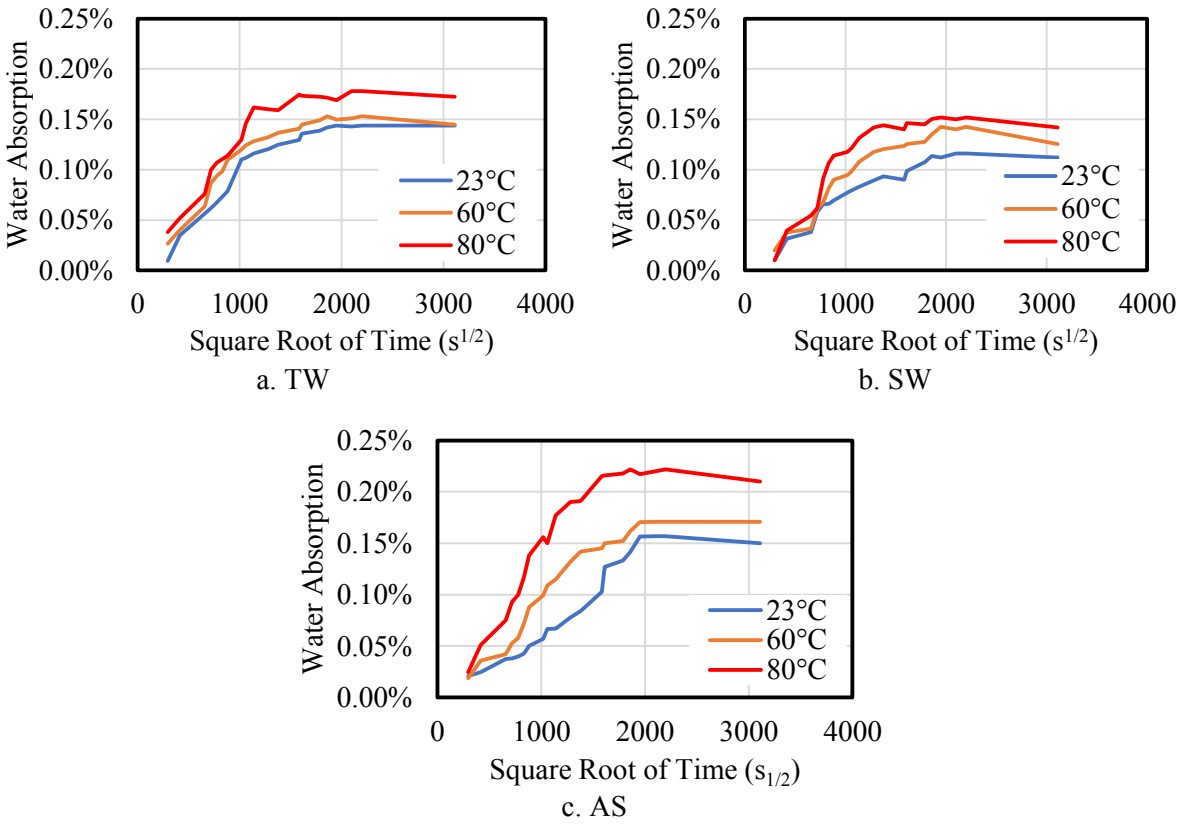

Figure 4: Moisture absorption process of GFRP bars conditioned at different solutions and temperatures.

Table 2 – Comparison of the peak moisture absorption (M_m) and apparent diffusivity (D)

Temperature (°C)	Tap Water		Saline Solution		Alkaline Solution	
	M_m (%)	D (×10^{-7} mm^2/s)	M_m (%)	D (×10^{-7} mm^2/s)	M_m (%)	D (×10^{-7} mm^2/s)
23	0.14	1.01	0.12	0.71	0.16	1.75
60	0.15	1.67	0.14	1.32	0.17	2.13
80	0.18	2.55	0.15	1.92	0.22	3.14

Interlaminar Shear Strength (ILSS)

The long-term properties of the bare and cement -embedded GFRP bars in different solutions was evaluated through investigation of their interlaminar shear strength (ILSS). Gooranorimi and Nanni (2017) and Benmokrane et al. (2018) used this property as a useful parameter for durability evaluation especially for GFRP bars in in-field conditions as the bars that can be extracted from the concrete core mostly has limited lengths.

All specimens failed because of the horizontal shear originated at the edge of the bars and developed along the length as shown in Figure 3b. A minor difference observed is the location of the inter-laminar shear crack along the bar's cross-section. In the control and conditioned GFRP bars after 28 and 56 days, the crack mostly occurred at the mid-depth of the bars. On the other hand, the crack in the bars conditioned after 112 days occurred below the mid-depth as shown in Figure 3b (right) indicating a weaker fiber–matrix interface in this location. This observed crack at the lower portion of the conditioned bars can be due to the bars already saturated with solution at the outermost resin rich surface, which was degraded and created a weak zones along which the transverse cracking could easily take place during testing.

Tables 3 and 4 summarise the average and standard deviation of the ILSS of bare and cement-embedded GFRP bars exposed to different solutions and temperatures, respectively. The low values of the standard deviation (maximum of 8.3%) suggest the good extraction of the bars, as Gooranorimi and Nanni (2017) and Benmokrane et al. (2018) indicated that this procedure is a major factor that may influence the ILSS of GFRP bars. The average ILSS of the unconditioned bars was 54.9 MPa with a standard deviation of 0.7 MPa. This is comparable to the properties reported by Benmokrane et al. (2017) in Table 1 as these bars were obtained from the same production lot.

Table 3 - Interlaminar shear strength in MPa of bare GFRP bars.

Temp (°C)	Tap Water			Saline Solution			Alkaline Solution		
	28 days	56 days	112 days	28 days	56 days	112 days	28 days	56 days	112 days
23	47.4 (0.1)	37.2 (0.7)	24.3 (0.7)	51.9 (0.8)	44.6 (0.5)	37.6 (0.4)	44.6 (0.2)	32.1 (0.2)	23.2 (0.8)
60	41.7 (0.3)	31.5 (0.7)	18.4 (1.2)	49.3 (1.6)	39.1 (0.4)	29.8 (0.6)	34.5 (0.5)	27.4 (0.4)	16.6 (0.7)
80	37.4 (0.7)	26.6 (0.6)	9.3 (0.8)	46.6 (0.3)	35.3 (0.7)	23.7 (0.6)	28.7 (2.4)	20.9 (0.9)	12.9 (0.9)

The numbers inside ( ) are the standard deviation

Table 4 – Interlaminar shear strength in MPa of cement-embedded GFRP bars.

Temp (°C)	Tap Water			Saline Solution			Alkaline Solution		
	28 days	56 days	112 days	28 days	56 days	112 days	28 days	56 days	112 days
23	50.3 (2.0)	49.3 (0.8)	48.1 (0.3)	52.5 (1.3)	50.8 (0.8)	49.7 (1.9)	47.5 (0.2)	45.9 (0.4)	44.1 (0.5)
60	48.8 (0.6)	47.0 (0.6)	45.6 (0.9)	50.8 (1.0)	49.4 (0.5)	47.7 (0.7)	43.4 (0.2)	41.5 (0.7)	40.3 (1.0)
80	43.5 (0.6)	41.5 (0.3)	38.5 (0.4)	47.3 (0.9)	46.1 (0.2)	44.6 (0.2)	41.3 (1.8)	39.1 (0.8)	36.3 (0.4)

The numbers inside ( ) are the standard deviation

Generally, the ILSS of the GFRP bars reported in Tables 3 and 4 decreases as the exposure temperature and duration increases in all exposure conditions. This can be attributed to the increase in percentage moisture uptake of the bars with exposure duration which leads to degradation of the fibre matrix interface, resulting in the decrease in the ILSS. When the bars absorbed moisture, the resin rich surface degrades and the bond between the matrix and fibers located at the outer part of the bar will gradually reduce and the bar resistance will start to decrease. While the water absorption of the GFRP bars was low (maximum of 0.22% for AS-conditioned bars after 112 days) indicating that only a very thin layer was affected by the solution, the softening of the resin at the edge of the bars was very critical under short-beam shear test as this location is subjected to high level of shear stress. Nkurunziza et al. (2005) highlighted that the interface between glass fibers and the resin controls the resistance of GFRP bars to different environments. However, the ILSS of cement-embedded GFRP bars were generally higher than that of the bare GFRP bars for similar immersion conditions. This behaviour can be attributed to the limited availability of the moisture around the bars and the lower temperature condition for the cement-embedded bars than the bare bars. Ceroni et al. (2006) indicated that the cut ends expose directly the fibers to external environment giving undesirable effects in the durability of the bars. The increased in temperature further increased the water absorption, which resulted in a faster degradation of the fiber and matrix interface leading to the decrease in the ILSS of the GFRP bars.

ILSS retention

The durability performance of the GFRP bars was appraised based from the ILSS retention after conditioning to different solutions and exposure durations. The ILSS retention was calculated by dividing the average ILSS shear strength for each bars reported in Tables 3 and 4 to that of the average property value for the reference specimen. Figure 5 shows the ILSS retention values of the conditioned bare GFRP bars while Figure 6 shows the ILSS retention values of the cement-embedded GFRP bars. From Figure 5, the following important information were observed:

- The AS is the most aggressive solution to GFRP bars affecting its ILSS. This is due to the highest absorption of the bars in this exposure condition. In the case of immersion in TW, the ILSS strength retention of bare GFRP bars at the end of 28 days immersion were 86%, 76% and 68% at 23, 60, and 80°C, respectively. For the same time of immersion, the ILSS retention were 94%, 90%, and 85%, respectively, for the bars conditioned in SS and were 81%, 63%, and 52%, respectively, for those conditioned in AS.
- At the end of 56-day immersion, the retention levels of the specimens immersed in tap water were 68%, 57%, and 48% for the 23, 60, and 80 °C cases, respectively, where as those immersed in saline solution yielded retention levels of 81%, 71%, and 64%, respectively. Retention levels of 58%, 47%, and 38%, respectively, were recorded for alkaline-conditioned specimens.
- At the end of 112-day immersion, the retention levels of the specimens immersed in tap water were 48%, 41%, and 29% for the 23, 60, and 80°C cases, respectively, where as those immersed in saline solution yielded retention levels of 69%, 54%, and 43%, respectively. Retention levels of 38%, 30%, and 23%, respectively, were recorded for alkali-conditioned specimens.

For cement-embedded GFRP bars, the following observations from Figure 6 suggest the following:

- The ILSS strength retention of unembedded GFRP bars at the end of 28 days immersion in TW were 92%, 89%, and 79% at 23°C, 60°C, and 80°C, respectively. For the duration of immersion, the ILSS retention were 96%, 93% and 86%, respectively, for the specimens conditioned in SS and were 87%, 79%, and 75%, respectively, for those conditioned in AS.
- At the end of 56-day immersion, the retention levels of the GFRP bars immersed in TW were 90%, 86%, and 76% for the 23, 60, and 80°C cases, respectively, where as those immersed in SS yielded retention levels of 93%, 90%, and 84%, respectively. Retention levels of 84%, 76%, and 71%, respectively, were recorded for AS-conditioned bars.
- At the end of 112-day immersion, the retention levels of the bars immersed in TW were 88%, 83%, and 70% for the 23, 60, and 80°C cases, respectively, where as those immersed in SS yielded retention levels of 91%, 87%, and 81%, respectively. Retention levels of 80%, 73%, and 68%, respectively, were recorded for AS-conditioned specimens. These results clearly that direct immersion in alkali solutions deteriorates the GFRP bars more severely than in the case of exposure to concrete alkali.

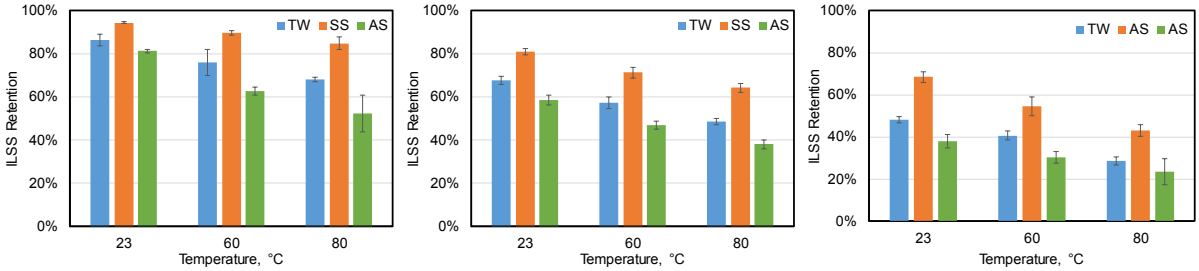

a. 28 days b. 56 days c. 112 days

Figure 5: Interlaminar shear strength retention of bare GFRP bars

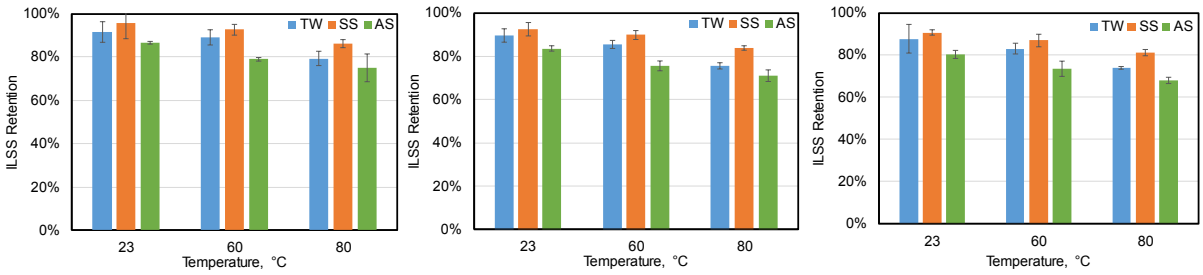

a. 28 days b. 56 days c. 112 days

Figure 6: Interlaminar shear strength retention of cement-embedded GFRP bars

The above experimental results clearly indicated the immediate impact of high temperatures on the degradation of ILSS of the GFRP bars. It was also observed that the ILSS retention of the GFRP bars decreases as the exposure temperature and duration increases in all exposure conditions. The significant degradation in ILSS could be explained by the degradation of the matrix at higher temperature which in turn could have affected the interface between the fibre and the matrix. The water molecules penetrated through the fiber-resin interface have a plasticization effect and hydrolysis reactions causing interfacial fracture. Moreover, the AS is found the most aggressive to GFRP bars affecting its ILSS. Chen et al. (2007) suggested that

the bond in the vinyl ester matrix is highly prone to the degradation at the presence of the free OH-ions in the alkaline solution by hydrolysis reactions due to the ester group leading to a leaching in the matrix and damaging in the glass fibers decreasing the interfacial bond strength. Furthermore, Micelli and Nanni (2004) indicated that the high pH of the pore water solution during the hydration of the concrete may cause the chemical attack of the glass fibers. This agrees with the findings of Nkurunziza et al. (2005) wherein they indicated that the most critical degradation of GFRP bars takes place in alkaline solution. Similar finding was observed by Wang et al. (2017) wherein they measured higher rate of degradation in the ILSS to solution with higher alkali-ion solution. However, the measured reduction in ILSS is significantly lower compared with the almost 90% reduction in ILSS in GFRP bars immersed in alkaline solution for 42days at 60^{o}C as measured by Micelli and Nanni (2004). On the contrary, Ashrafi et al. (2018) measured a maximum reduction of 15% in the ILSS of E-glass FRP bars subjected to water vapour condensation after 3000 hours as this conditioning only affected the very thin matrix rich surface of the bars. Similarly, Benmokrane et al. (2017) measured only a 12% decrease in ILSS for a 9.5 mm diameter GFRP bar after conditioning in an alkaline solution for 90 days at 60^{o}C.

The decrease in the ILSS retention of GFRP bars exposed to TW and SS are in agreement with the evaluation conducted by D'Antino et al. (2018) that vinylester-based GFRP bars embedded within concrete and conditioned in tap water and saline solution at 50-60^{o}C showed significant strength decrease with increasing exposure time. Wang et al. (2017) measured only a 50% retention in the interlaminar shear strength of GFRP bars exposed in seawater solution at 55^{o}C for 84 days. While researchers (Robert et al. 2009; Robert and Benmokrane 2013) have indicated that tapwater and saltwater have similar effects on the durability of the GFRP bars, the results of this study suggest a higher decrease in ILSS exposed in tapwater than in seawater. D'Antino et al. (2018) have a similar observation wherein GFRP bars conditioned in salt solution were less degraded than those conditioned with plain water at the same temperature. This can be due to the higher moisture uptake of the GFRP bars in TW than in SS as shown in Figure 3. This can be also explained by the large salt molecules in the saline solution slowing the diffusion of water by blocking the paths which water diffuses into the bars as was also found by Mouzakis et al. (2008). Almusallam et al. (2012) further indicated that the lower water absorption of GFRP bars in SS than TW can be attributed to the formation of very thin layer of salt on the specimen surface, especially at higher temperature which decreases the diffusion rate of the solution into the GFRP bars. In all exposure temperatures considered in this study, the rate of diffusion of GFRP bars exposed in SS was lower than that of TW. It is also worth noting that the works of Robert et al. (2009) and Robert and Benmokrane (2013) considered the tensile strength as an indicator of degradation. This property is governed more by the properties of the fibres and not the matrix, which can be better evaluated by ILSS test.

For cement-embedded GFRP bars, it can be noticed that the reduction in ILSS increased gradually with time. In contrast, a significant decrease even only after 28 days can be observed for bare GFRP bars especially for bars exposed in AS. For example, the bare GFRP bars retained only 63% of its ILSS while cement embedded bars retained 79% at 60^{o}C exposure in AS. The 21% decrease in ILSS for cement embedded bars is almost equal to the 23% decrease in the ILSS measured by Gooranorimi and Nanni (2017) in 15.9 mm diameter GFRP bars extracted from a concrete bridge deck after 15 years of service. However, it is important to note that only one extracted sample was tested by these researchers and insufficient to prove the

reliability of the test results. Similarly, Micelli and Nanni (2004) estimated that the alkaline exposure of GFRP bars for 21 days at 60ºC would correspond respectively to 14 years in a real concrete structure. The higher ILSS retention of cement embedded GFRP bars was due to the cement which may not be completely saturated, and the moisture from outside of the concrete is not in direct contact with the bars. The cement cover minimises the water absorption of the GFRP bars whereas the bare GFRP bars are completely immersed in solution that wet all the bar external surface. As a result, the reaction of decomposition in the GFRP bars embedded in the cement would be slower because of the absence of oxidation reaction of the polymer matrix.

SEM and FTIR Observations

Scanning-electron-microscopy (SEM) observations were performed to assess the microstructure of the GFRP bars before and after conditioning after 112 days using the JEOL JSM-840A SEM (JEOL, Akishima, Tokyo, Japan). All of the specimens observed under SEM were cut, polished, and coated with a thin layer of gold–palladium using a vapor-deposit process. SEM observations were performed in both the cross-section of the bars and at the fibre-matrix interface. Similarly, Fourier Transformed Infrared Spectroscopy (FTIR) was conducted to study the changes in the chemical composition of the matrix at the bar surface. These observations were implemented to determine the potential degradation of the polymer matrix, glass fibers, or interface, as applicable, due to the penetration of the solution. The aim was to link these observations to the possible evolution of ILSS and chemical composition of the bars after conditioning.

SEM

Figure 7 shows the SEM observation at the cross section of the bars at 2500 times magnification. There was no visible difference observed between the bars and the cement embedded bars and exposed in different solutions. This can be due to the bar not under the stress so the fibers and matrix interface is still intact. Moreover, no pores, air bubbles were observed indicating the high quality of the manufacturing process.

SEM was also performed on the fracture zones near the ends of the GFRP bars conditioned for 112 days after the short beam testing to investigate the mechanisms of failure at the fiber-matrix interface as shown in Figure 8. The SEM shows that the fracture of the surfaces are dominated by matrix fracture as the matrix layer at the surface that covers and protects the glass fibers was lost in some areas. In all specimens, no fibre damage in the internal section of the bar was observed. As compared to the bare GFRP bars exposed to TW and SS (Figures 8a and 8b, respectively), which shows resin adhering to fibers, i.e. a good interface, the resin left on the fibre surface of the bars exposed to AS became less indicating decreased bonding strength between fibre and resin. Figure 8c shows some of the fibres are smooth and almost no resin residues, which indicates that the rupture occurred partly at the interface. In contrast, the fiber surface of the cement embedded GFRP bars had more resin coverage than those bare GFRP bars but still could have lost a certain adhesion. This observation explains the lower ILSS retention of the bare GFRP bars compared to that of the cement embedded bars after conditioning. Moreover, a lot of residual resin covers on the fibre surface was observed for cement embedded bars exposed to TW and AS (Figures 8d and 8e, respectively), which suggests a better bonding between the fibre and vinyl-ester resin than the bars exposed to AS (Figure 8f). This observation also suggests that the integrity of the fiber and matrix interface can be better evaluated by observing the fracture surface than at the ends of the GFRP bars.

The observed damage of the fibre-resin interface and decrease in the ILSS was due to the penetration of the fluid that resulted in a moderate moisture content after immersion. The moisture absorbed by the bars, combined with the temperature of exposure, induces stress in the material with consequent damage at their interface decreasing the ILSS strength with time. Mouzakis et al. (2008) indicated that absorbed water can disrupt the interfacial bonds between the fibre and the matrix. Moreover, Ceroni et al. (2006) indicated that a deterioration of this interface reduces the capacity of load transfer between fibers resulting in the decrease in the mechanical properties. Davalos et al. (2011) highlighted that the fibrer-matrix interface integrity is critical for load transfer between fibers, and the interface degradation weakens the composite materials. Moreover, Nkurunziza et al. (2005) indicated that the chemical bond between the coupling agent and the surface of the glass fibres is not stable in the presence of moisture and alkalis. When the moisture and the alkalis was absorbed by the bars, this bond is destroyed gradually causing damage to the interface, and reducing the stress transfer efficiency between the fibers and matrix within the composite. This presence of water combined with a high pH levels considerably affects the physical and chemical degradation at the fibre-matrix interface.

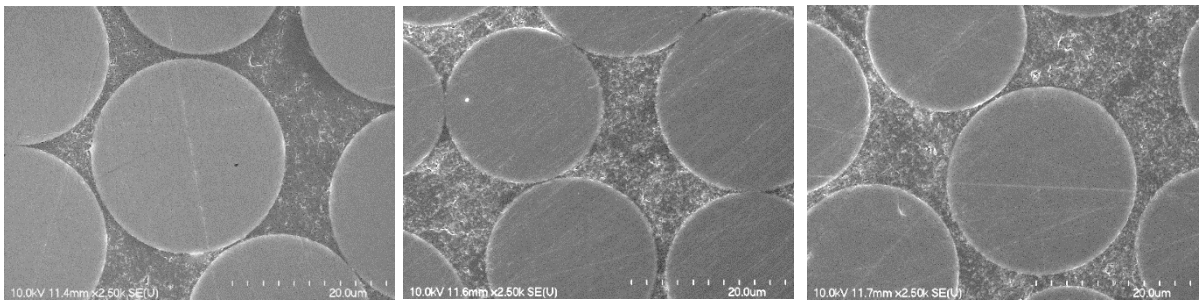

(a) TW (b) SS (c) AS

Figure 7 : SEM observations at the cross section of the bars

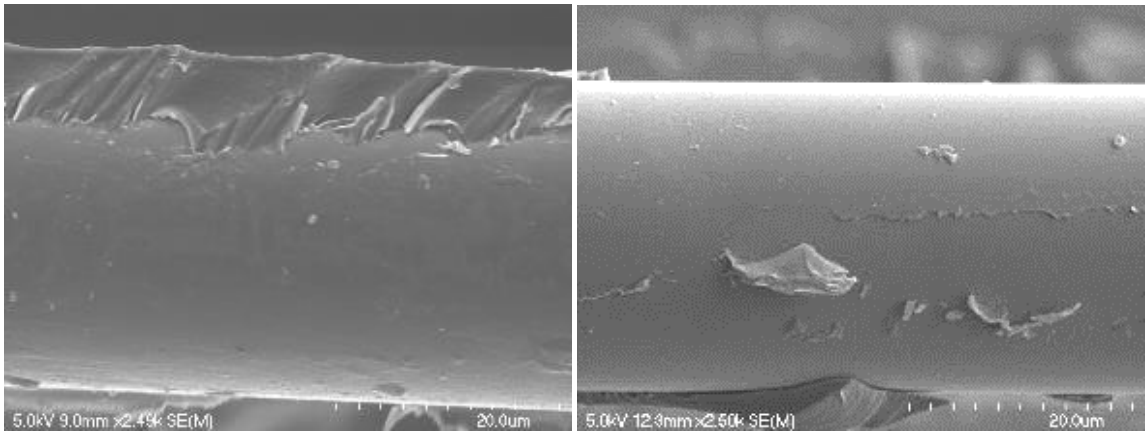

(a) TW (bare GFRP bars) (b) SS (bare GFRP bars)

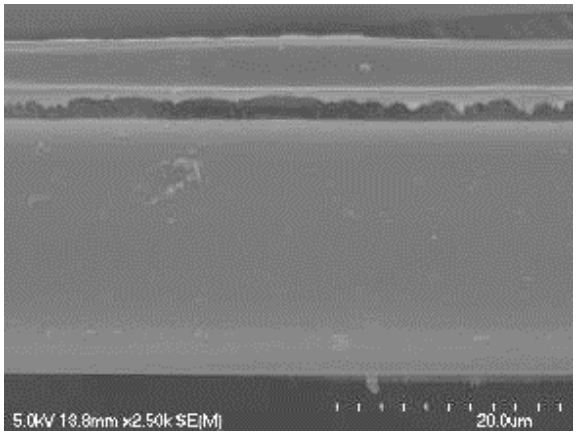

(c) AS (bare GFRP bars)

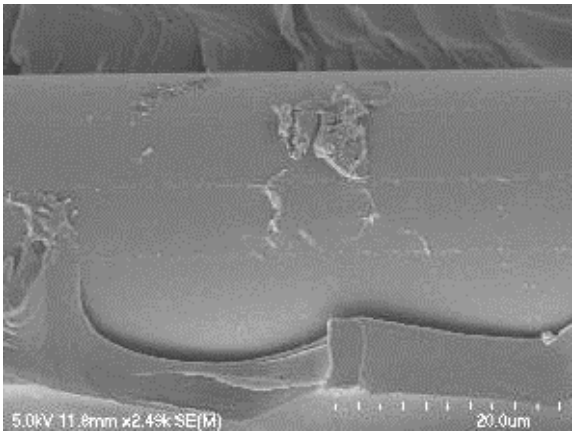

(d) TW (cement embedded)

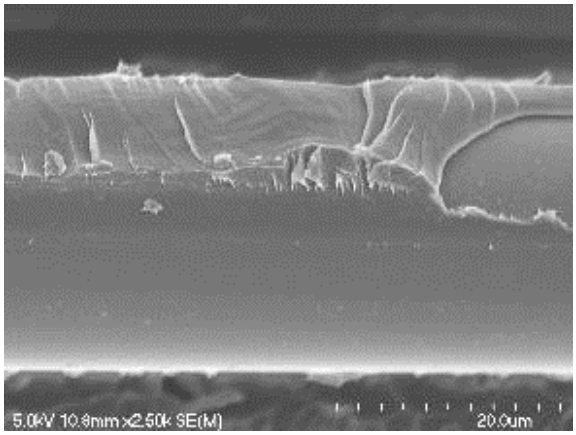

(e) SS (cement embedded)

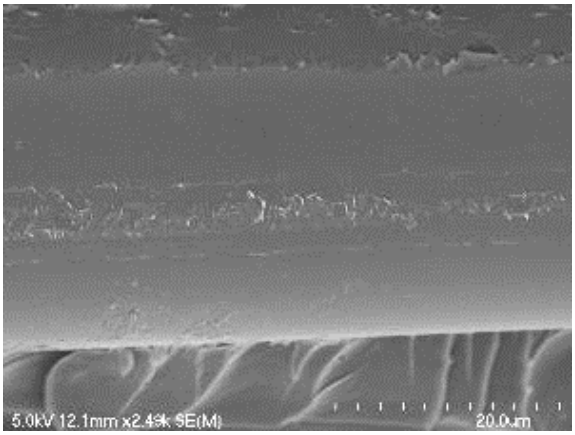

(e) AS (cement embedded)

Figure 8: SEM observations at the failure surface of conditioned GFRP bars

FTIR

The FTIR spectra of the GFRP bars recorded using a Nicolet Magma 550 spectrometer is shown in Figure 9. In both the bare GFRP bars (Figure 9a) and cement embedded bars (Figure 9b), the FTIR spectra was focused on OH units around 3500 cm^{-1} and CH groups (around 2900 cm^{-1}). When there is a degradation by hydrolysis, the OH peak dramatically increase as compare to the CH peak which remains constant. The hydroxyl peak did not show any significant changes which indicates that no significant hydrolysis of GFRP bars occurred except for the relatively higher intensity of the O-H stretching band at 3400 cm^{-1} for the bare GFRP bars exposed in AS. Chin et al. (2001) suggested that this spectral change is consistent with ester hydrolysis, in which ester functional groups are converted to hydroxyl and carboxylic acid products. However, this higher intensity was only observed at the bar surface indicating that the water absorption was only concentrated in the thin resin rich area of the GFRP bars. This indicates that ageing might have occurred on the surface of the GFRP bars. However, it is also important to note that the O-H stretching may not also be due to hydrolysis. Vinyl ester naturally contains OH, and if non-evaporated water or alkalis are present inside the bars, the amount of OH will increase too. This degradation in the materials explained the fracture fibre and matrix interface observed under the SEM and the significant loss in the ILSS of the bare GFRP bars exposed in the alkaline solution.

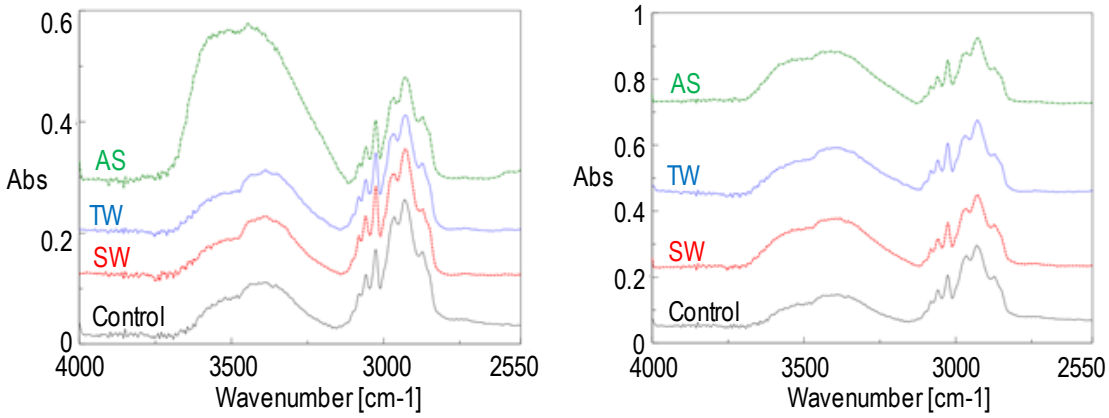

(a) GFRP bars (b) Cement embedded bars

Figure 9 : FTIR of GFRP bars

Prediction of long-term behaviour and service life for ILSS of GFRP bars

Aiello et al. (2006) indicated that a reliable prediction of a long-term behaviour of civil infrastructure upon the action of environmental factors is a complex problem. Similarly, Wang et al. (2016) highlighted that the durability of fiber-reinforced polymers under different environments is difficult to ascertain because of non-standardization of various conditioning effects and variation in material constituent. This requires accelerated aging through hygrothermal exposure for the long-term assessment of materials durability and relies on the superposition of temperature and moisture to enhance and speed up environmental degradation. Moreover, Davalos et al. (2011) highlighted that only a few studies were directed to the development of life-cycle durability prediction models for FRP bars in concrete environment. Naya et al. (2013) indicated that the most accurate method is the Arrhenius method for materials exposed to temperature less than its glass transition temperature. Thus, the long-term interlaminar shear strength performance of GFRP bars investigated in this study was predicted in accordance with Arrhenius relation and following the procedure implemented by Bank et al. (2003). As a requirement, at least three elevated temperatures and three exposure durations are necessary to perform an accurate prediction based on Arrhenius law (Robert and Benmokrane 2013), which was conducted in this study.

Arrhenius model

Arrhenius equation is used to express the degradation rate for materials with time as denoted by Nelson (2009) using Equation 3:

$$k = A \times e^{\left(\frac{-E_a}{RT}\right)} \qquad \text{Equation 3}$$

where k is the degradation rate $(1/time)$, A is a constant based on material properties, E_a is the activation energy, R is the universal gas constant, and T is the temperature in Kelvin. The basic assumption in this prediction model is that the material properties of the GFRP bars are not affected by the temperature during exposure and the rate of degradation is accelerated with the increase in temperature. Therefore, analysing procedures to identify the factors in the rate of degradation consist of transforming Eq. (3) to produce a linear equation between the time

($t = 1/k$) and the inverse of temperature ($1/T$) by taking the natural logarithm for the two sides of the equation, as shown in Equation 4:

$$\ln(\frac{1}{k}) = \frac{-E_a}{R}\left(\frac{1}{T}\right) + \ln(A) \qquad \text{Equation 4}$$

Afterwards, the Arrhenius method is carried out by plotting the natural logarithm of time needed to reach 90%, 80%, 70%, and 60% strength retention (SR) of the ILSS of the GFRP bars with the inverse temperature ($1000/T$) in Kelvin to obtain the regression coefficient ($\frac{E_a}{R}$) value. This value was expressed by the slope of the linear equations as can be seen in Figure 10 for bare bars and Figure 11 for embedded bars in concrete, immersed in different liquid solutions. Regression analyses were done to determine the line-of-best-fit as shown in these figures. The straight lines were nearly parallel to each other, indicating that the accelerated aging tests were valid, and this model may be applied to describe the ILSS degradation of GFRP bars. Moreover, the R^2 of the regression line is at least 0.95 which is well above 0.80 as indicated by Benmokrane et al. (2016). The average of these slopes represent the $\frac{E_a}{R}$ values.

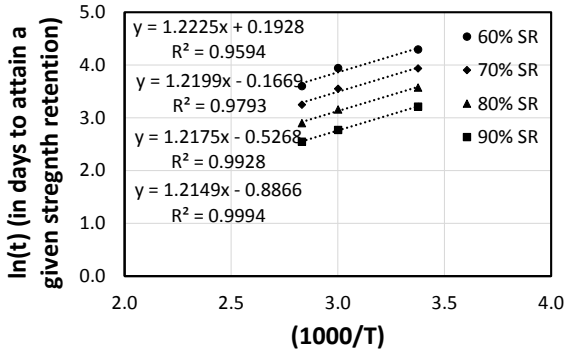

(a) bare bars in TW

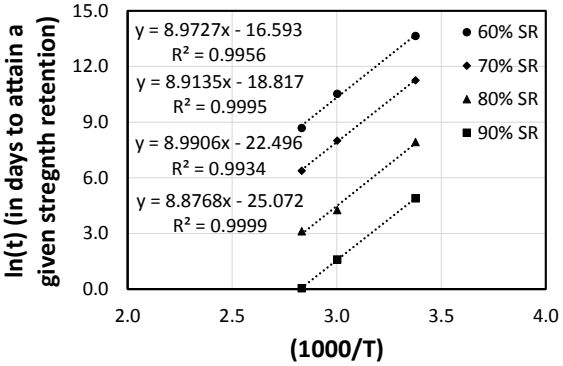

(d) embedded bars in TW

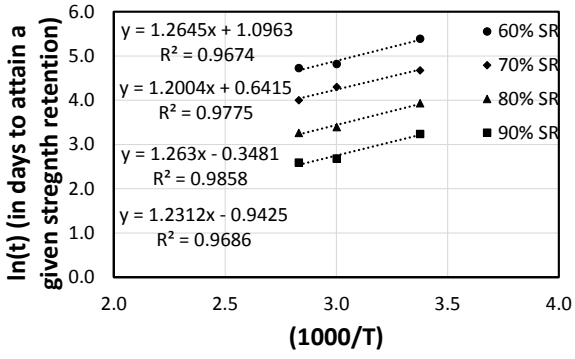

(b) bare bars in SS

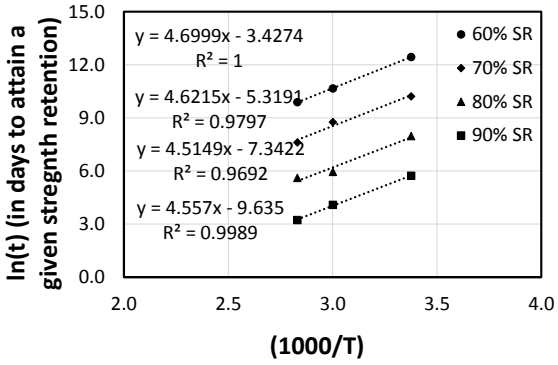

(e) embedded bars in SS

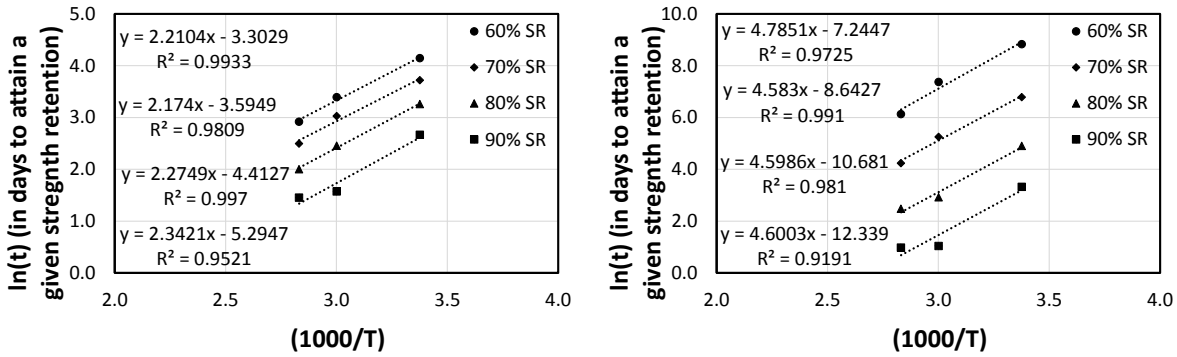

(c) bare bars in AS (f) embedded bars in AS

Figure 10: Arrhenius plots for the service life of the bare bars and embedded GFRP bars in concrete

The regression coefficient ($\frac{E_a}{R}$) were used to determine the relative time shift factor (TSF) for all conditioning cases with respect to two different temperatures [See Eq. (5)] as suggested by Dejke (2001). In Eq. (5), t_1 and t_2 (days) are the time required to reach a certain strength retention (SR), k_1 and k_2 are the degradation rates corresponding to t_1 and t_2, respectively, T_{ref} and T_0 are the reference temperature and the exposure temperature (Kelvin), respectively. Figure 12(a) illustrates the procedure on finding the TSF using Equation (5) based on the corresponding exposure temperature. In this equation, the $\frac{E_a}{R}$ values are determine from Figures 10 and 11 where T_{ref} is taken as the room temperature of 23°C to evaluate the TSF for the target temperature T_0. For example, the TSF for an embedded GFRP bar in concrete immersed in TW at 60°C is 28.64 as shown in Figure 12(a). Following this procedure, the corresponding TSF values for all exposure conditions and temperatures considered in this study are tabulated in Table 5. On the other hand, the TSF for an exposed temperature of 30°C shown in Figure 12(b). A temperature of 30ºC is considered as this is the average annual temperature in Australia. Table 6 shows all values for embedded bars in concrete at 30°C with respect to 23°C. The main purpose of TSF is to transform the time taken in accelerated tests at a known exposure condition and temperature, and correlate this with the actual service life of GFRP bars inside concrete. In this study, the reference temperature was chosen at the room temperature condition of 23°C. Accordingly, $\frac{E_a}{R}$ and TSF values for all conditioning cases are tabulated in Table 5. As can be noticed from Table 5, the $\frac{E_a}{R}$ values for embedded GFRP bars in concrete is much higher compared to bare bars indicating that the required activation energy to cause the degradation for the bars inside concrete is higher. This also means that the cement embedded bars have a lower degradation rate compared to the GFRP bars which were directly immersed into the solutions, which explains the benefit of the surrounding concrete cover in extending the durability of the GFRP bars in the actual structures.

$$TSF = \frac{t_1}{t_2} = \frac{k_2}{k_1} = \frac{A \times e^{(\frac{-E_a}{RT_0})}}{A \times e^{(\frac{-E_a}{RT_{ref}})}} = e^{(-\frac{E_a}{R})(\frac{1}{T_0} - \frac{1}{T_{ref}})} \quad \text{Equation 5}$$

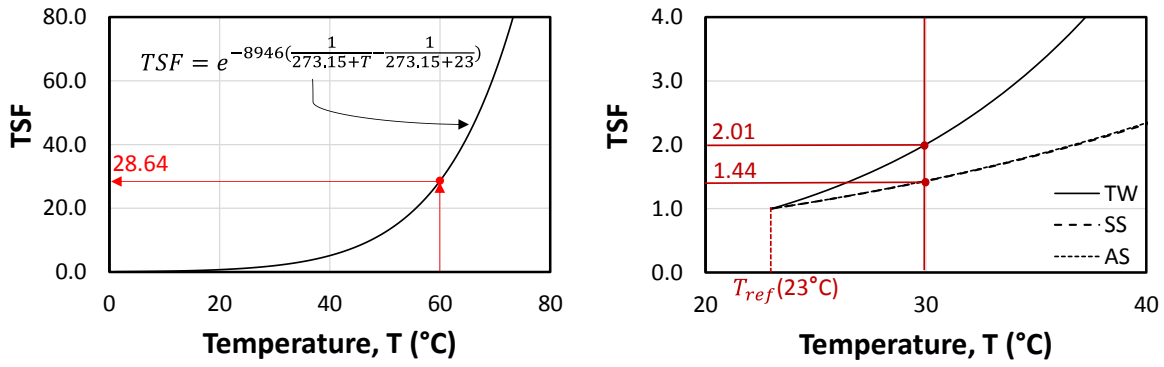

(a) TW at 60°C (b) Different exposure at 30°C

Figure 12: Illustration of evaluating the TSF for embedded GFRP bar in concrete

Table 5: $\frac{E_a}{R}$ and TSF values for all conditioning cases

Bar case	Accelerated agent	$\frac{E_a}{R}$	TSF 23 °C	TSF 60 °C	TSF 80 °C
Bare GFRP bars	TW	1217	1.00	1.58	1.94
	SS	1240	1.00	1.59	1.97
	AS	2250	1.00	2.33	3.41
Embedded GFRP bars	TW	8946	1.00	28.64	131.06
	SS	4599	1.00	5.61	12.26
	AS	4642	1.00	5.70	12.55

Predicting the long-term behaviour and constructing master curves

A number of methods were suggested to predict the long-term behaviour of the GFRP bars following accelerated tests (Bank, et al., 2003, Dejke, 2001). However, Chen et al. (2006) and Ali et al. (2019) suggested that the better way of getting a more precise and accurate prediction is to develop a master curve containing a plot for all the data used for analysis. This master curve consist of the time required to reach a specific SR corresponded to its TSF considering the effect of temperature. Accordingly, Figures 13 and 14 show the master curves at a temperature of 23ºC for the bare and cement embedded bars at different conditioning environment implemented in this study. These curves show the SR in % in the y-axis against time, t in days in the x-axis. It can be observed that master curves can be expressed by a logarithmic equation with R^2 of at least 0.94. This means that the proposed SR versus time model by (Bank, et al., 2003) is valid and resulted in a good prediction for the long-term behaviour following Eq. (6) in its general form, where a and b are a regression constants.

$$SR = a\ln(t) + b \qquad \text{Equation 6}$$

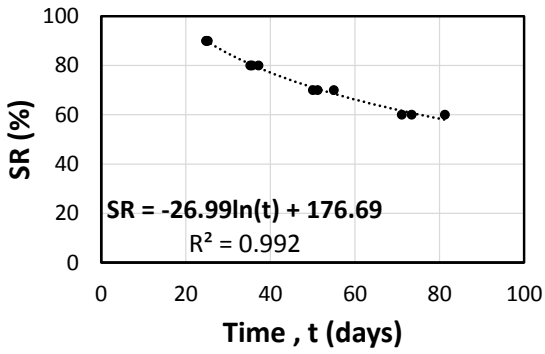

(a) bare bars in TW

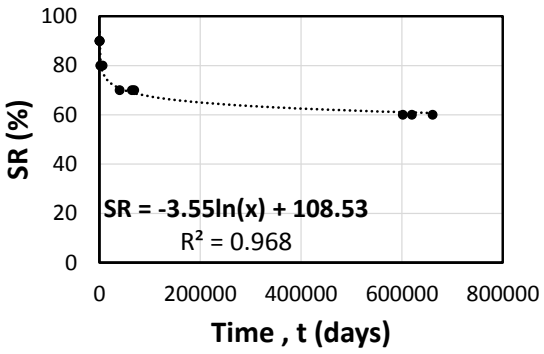

(d) embedded bars in TW

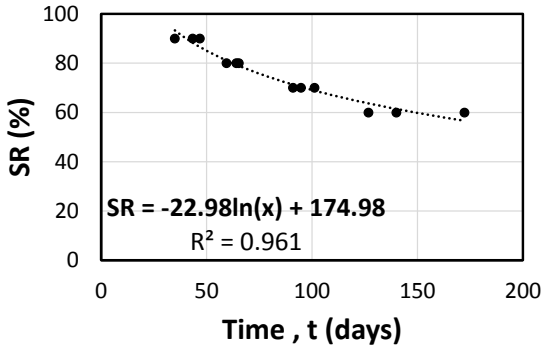

(b) bare bars in SS

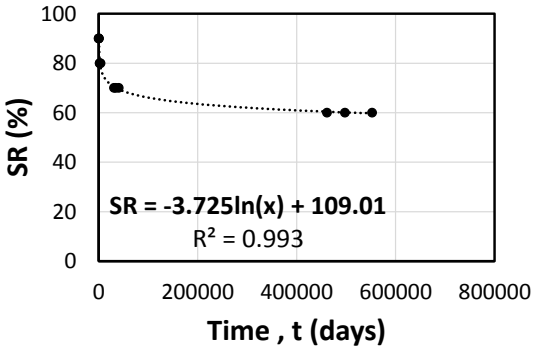

(e) embedded bars in SS

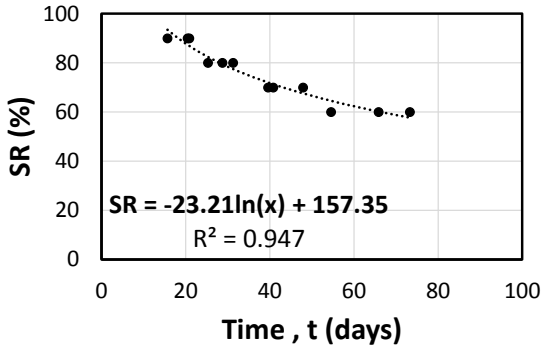

(b) bare bars in AS

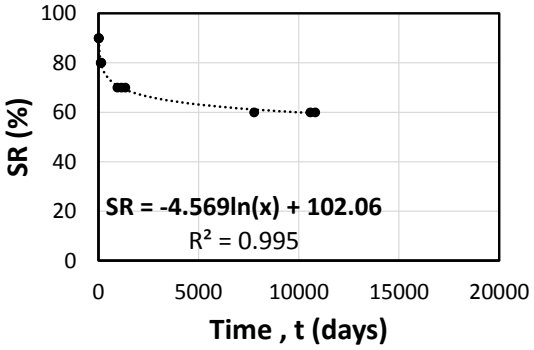

(f) embedded bars in AS

Figure 13: Master curves for bare bars and embedded bars in concrete at 23 C°

Equivalent service life for GFRP bars in concrete environment

The strength retention measured for the bare GFRP bars exposed in the different solutions at different temperature and exposure time was correlated to the strength retention of the cement embedded bars to determine the equivalent service life for GFRP bars in the concrete environment. As an example, the prediction of the service life of the GFRP bars in the concrete environment was performed at a mean annual temperature of 30ºC, which is the average annual temperature in Australia. This prediction was made for ILSS strength retention as a function of service life to a maximum of 100 years as bridge infrastructures in Australia are designed to be in service for this length of time (Austroads, 2016). Accordingly, master curves of the SR of the GFRP bars in concrete structures during its service life at 30°C exposed to different

exposure environments (TW, SS, and AS) were created (see Figure 15). These master curves were constructed following the procedures described in developing Figures 15 and 16 but modified using the corresponding TSF listed in Table 6. As can be seen from the graphs, the GFRP bars exposed in TW and SS can retain 60% of their ILSS up to 900 years and 1050 years, respectively while GFRP bars in AS can retain 60% of its ILSS after 20 years in service.

Table 6 - TSF values for embedded bars in concrete at 30°C with respect to 23°C

	TW	SS	AS
TSF	2.01	1.43	1.44

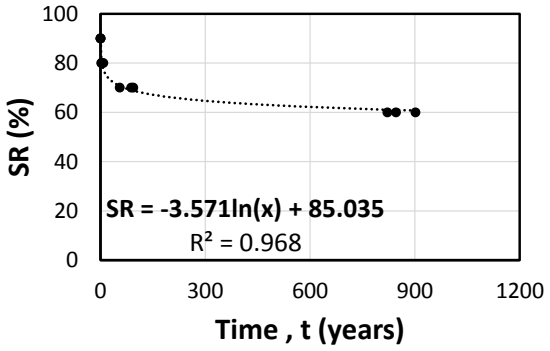

(a) TW

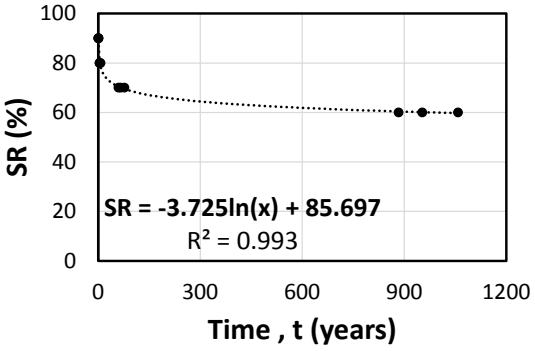

(b) SS

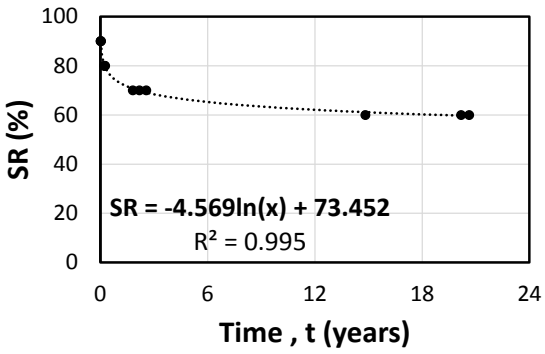

(c) AS

Figure 15: Master curves for GFRP bars exposed at different environments at 30°C

From the master curves in Figure 15, the SR of the GFRP bars in concrete structures exposed to different environment at an annual average temperature of 30ºC up to 100 years was established as shown in Figure 16. As highlighted in previous sections, the service life of the GFRP bars in actual concrete structures was predicted from the accelerated aging test results by correlating the strength retention of the bare GFRP bars to that of the cement embedded bars. As a first step, the SR value for the bare bars was calculated using the curve fitting of the master curves in Figure 12 and the corresponding TSF value was calculated using Eq. (3). Next, the master curve in Figure 13 for cement embedded bars was developed and modified using the corresponding TSF. If the annual average temperature is at 30°C, then the master curve in Figure 15 can be adopted directly. For example, the expected SR of a bare GFRP bar submerged in SS and exposed to 60°C for 56 days using the master curve in Figure 14b is:

$SR = -22.98 \ln(t \times TSF) + 174.98$, where TSF is 1.59 in Table 5.

$SR = -22.98\ln(56 \times 1.59) + 174.98 = 71.82\%$

The equivalent service life for these GFRP bars in concrete structures exposed in alkaline environment at an annual average temperature of 30°C using the master curve in Figure 14c, i.e. ($SR = -4.569\ln(t) + 73.452$) where *SR* is 71.82% is $t = 1.429$ years.

Another example, a bare GFRP bar submerged in TW for 30 days and exposed to 80°C, the expected SR for this bar following the curve fitting in Figure 14a is:

$SR = -26.99\ln(t \times TSF) + 176.69$, where TSF is 1.94 in Table 5.

$SR = -26.99\ln(30 \times 1.94) + 176.69 = 67.01\%$

The equivalent service life of these in an actual concrete environment at an annual average temperature of 30°C and exposed to sea water (SS) using Figure 14b ($SR = -3.725\ln(t) + 109.01$) is $t = 150.9$ years, which is more than the service life (100 years) of the GFRP bars in concrete structures. An accelerated test for bare GFRP bars submerged in AS for 20 days and exposed to a temperature of 70°C will have a SR of 63.67% following the master curve in Figure 13c:

$SR = -23.21\ln(t \times TSF) + 157.35$, where TSF can be calculated using Eq. (3).

$TSF = e^{(-2250)(\frac{1}{273.15+70} - \frac{1}{273.15+23})} = 2.831$

$SR = -23.21\ln(20 * 2.831) + 157.35 = 63.67\%$

The equivalent service life of these bars in actual concrete environment at an average annual temperature of 30°C in an alkaline environment using Figure 14c, i.e. ($SR = -4.569\ln(t) + 73.452$) is $t = 8.51$ years.

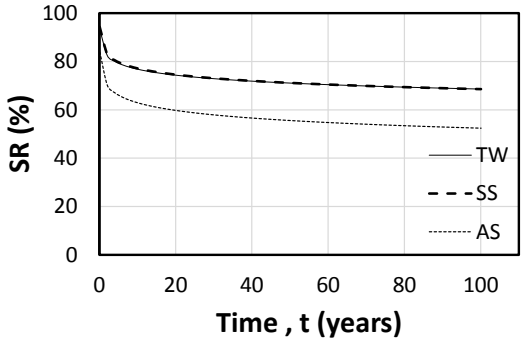

Figure 16: Service life of GFRP bars in concrete structures at 30°C

As a summary, the GFRP bars will retain 54% of its ILSS when exposed to alkaline environment and nearly 68% for bars exposed in tapwater and seawater after 100 years of service (Fig. 15). These results further shows that the GFRP bars will last longer in the concrete environment than directly exposed to the simulated concrete environmental conditions. These findings support the observations by Benmokrane et al. (2018) wherein they measured a maximum 16% reduction ILSS in vinyl-ester GFRP bars extracted from the concrete bridge barriers after 11 years in service. The slightly lower ILSS reduction from the field study than this laboratory study can be due to the bars were well protected by concrete as the concrete cover is at least 65 mm. Similarly, the pH value measured from the core samples is only 12.3,

which is lower than the pH of the cement used in this study. Nonetheless, these results clearly showed that the natural conditions are generally less aggressive to GFRP bars aging due to lower temperature and humidity conditions than constant elevated temperature and continuous contact and complete saturation in the solution of GFRP bars in the accelerated exposure tests. Finally, these findings confirm the conclusions by Wang et al. (2017) that the long-term predictions for FRP bars directly placed in the simulated solutions are too conservative compared with the field results wherein the bars are embedded in concrete.

CONCLUSIONS

This study comparatively evaluated the durability of GFRP bars in concrete and in simulated concrete environment through the investigation of their interlaminar shear strength. It focuses on the evaluation of the physical, mechanical and micro-structural properties of GFRP bars under high moisture, saltwater and alkali environments. From the results of this work, the following conclusions can be drawn:

- The percentage water uptake and the apparent diffusivity of the GFRP bars were strongly dependent on the type of solution and temperature, with the percentage water absorption and apparent diffusivity higher for high than low temperature exposure. For similar degree of temperature exposure, the GFRP bars conditioned in the alkaline solution has the highest moisture uptake and apparent diffusivity rate followed by the bars conditioned in tap water with the saline solution the least.
- The interlaminar shear strength of the GFRP bars decreased as the exposure temperature and duration increased with the ILSS of cement-embedded GFRP bars were generally higher than that of the bare GFRP bars for similar immersion conditions.
- The alkaline solution is more aggressive to GFRP bars affecting its interlaminar shear strength than tapwater and saline solution. After 112 days conditioning at 60^{o}C, the bare GFRP bars retained exposed to this solution retained only 30% of its interlaminar shear strength with the bars exposed to tapwater and saline solution retaining 41% and 54%, respectively.
- Direct immersion in solution deteriorates the interlaminar shear strength of GFRP bars more severely than in the case of cement embedded bars. After 112 days conditioning at 80^{o}C, the cement embedded GFRP bars exposed in alkaline solution can retain 68% of its interlaminar shear strength compared to only 23% for bare GFRP bars.
- SEM showed that the fiber surface of the cement embedded GFRP bars had more resin coverage than the bare GFRP bars. Likewise, more residual resin covers on the fibre surface was observed for the GFRP bars exposed to tap water and saline solution than in alkaline solution suggesting a better bonding between the fibre and vinyl-ester resin.
- The FTIR spectra did not show any significant changes in the polymers chemical structure except for the relatively higher intensity of the O-H stretching band for the GFRP bars directly immersed in the alkaline solution. However, this higher intensity was only observed at the bar surface indicating that the water absorption was only concentrated in the thin resin rich area of the GFRP bars.
- Based on the Arrhenius relation, the required activation energy to cause the degradation for GFRP bars inside concrete is higher than the bare GFRP bars directly immersed into different accelerated aging solutions, which explains the benefit of the surrounding concrete cover in extending the durability of the GFRP bars in the actual structures.

- Master curves and time shift factor to correlate the strength retention of the the accelerated aging test using bare GFRP bars to the equivalent service life for GFRP bars in the concrete environment were developed. Based on this correlation, the GFRP bars in actual concrete structures will retain up to 54%, 68% and 68% of its ILSS after 100 years of service at an annual average temperature of 30^{o}C when exposed to alkaline environment, tapwater and saline solution, respectively.

The results from this work provided a good representation and comparison of the long-term properties and durability performance of GFRP bars in simulated and actual concrete environment. Furthermore, the short shear beam shear test gave a straightforward and reliable indication of the resistance of the fiber–matrix of GFRP bars exposed in different environmental conditions. However, a comparative study to relate the interface property of GFRP bars using short-beam shear test to the longitudinal properties can lead to a simpler and more practical assessment of the durability and long-term performance of GFRP bars in concrete environment.

References:

ASTM D7705/D7705M – 12: Standard Test Method for Alkali Resistance of Fiber Reinforced Polymer (FRP) Matrix Composite Bars used in Concrete Construction

ASTM D 1141-98 (2013): Standard Practice for the Preparation of Substitute Ocean Water

ASTM D4475 -02 (2016): Standard Test Method for Apparent Horizontal Shear Strength of Pultruded Reinforced Plastic Rods by the Short-Beam Method.

ASTM D570 (2010): Water absorption of plastics. *ASTM D4972-13*, ASTM International, West Conshohocken, Philadelphia, Pa 19103.

ASTM Standard ASTM D4972 (2013). Standard Test Method for pH of Soils. *ASTM D4972-13*, ASTM International, West Conshohocken, Philadelphia, Pa 19103.

Adams, D. 2018. What is the most important type of mechanical test for composites? Composites World 2018; 4(1), 10-11.

Aiello, M.A., Leone, M., Aniskevich, A.N., Starkova, O.A. (2018). Moisture effects on elastic and viscoelastic properties of CFRP rebars and vinylester binder. *ASCE Journal of Composites for Construction*, 18, 686-691.

Ali, A. H., Mohamed, H. M., Benmokrane, B., ElSafty, A., and Chaallal, O. (2019). "Durability performance and long-term prediction models of sand-coated basalt FRP bars." Composites Part B: Engineering, 157, 248-258.

Almusallam TH, Al-Salloum YA, Alsayed SH, El-Gamal S, and Aqel M. Tensile properties of glass fiber-reinforced polymer bars embedded in concrete under severe laboratory and field environmental conditions. Journal of Composite Materials 2012; 47(4), 393-407.

Ashrafi, H, Bazli, M, Oskouei AV, Bazli, L. (2018). Effect of Sequential Exposure to UV Radiation and Water Vapor Condensation and Extreme Temperatures on the Mechanical Properties of GFRP bars. *ASCE Journal of Composites for Construction*, 22(1), 04017047-1-17.

Austroads (2016).Realising 100-years Bridge Design Life in an Aggressive Environment: Review of the Literature. Austroads Technical Report AP-T313-16.

Bank, L. C., Gentry R.T., Thompson, B.P., Russell, S.J. (2003). A Model Specification for FRP Composites for Civil Engineering Structures. *Construction and Building Materials*, 17(6-7), 405-437.

Belarbi A. and Wang, H. (2012). "Durability of FRP bars embedded in fiber-reinforced concrete." *ASCE Journal of Composites for Construction*, 16(4), 371-380.

Benmokrane B, Ali A, Mohamed H, Robert M, and ElSafty A. (2017a). "Durability Performance and Service Life of CFCC Tendons Exposed to Elevated Temperature and Alkaline Environment". *ASCE Journal of Composites for Construction*; 20(1), 04015043-1:13.

Benmokrane B, Manalo A, Bouhet J-C, Mohamed K, and Robert M. (2017b). "Effects of diameter on the durability of glass-fiber-reinforced-polymer (GFRP) bars conditioned in alkaline solution." *ASCE Journal of Composites for Construction*; 21(5), 04017040-1:12.

Benmokrane B, Ali AH, Mohamed HM, ElSafty A, Manalo A. Laboratory assessment and durability performance of vinyl-ester, polyester, and epoxy glass-FRP bars for concrete structures. Composites Part B. 2017; 114: 163-174.

Benmokrane B, Nazair C, Loranger M, and Manalo A. (2018). "Field Durability of Vinyl-Ester-Based GFRP Rebars in Concrete Bridge Barriers". *ASCE Journal of Bridge Engineering*, 23(12), 04018094-1-13.

Ceroni, F, Cosenza, E, Gaetano, M, Pecce, M. Durability issues of FRP bars in reinforced concrete members. Cement and Concrete Composites 2006; 28, 857-868.

Chen, Y., Davalos, J. F., and Ray, I. (2006). "Durability prediction for GFRP reinforcing bars using short-term data of accelerated aging tests." *Journal of Composites for Construction*, 10(4), 279-286.

Chin, J.W., Aouadi, K., Haight, M.R., Hughes, W.L., and Nguyen, T. (2001). "Effects of water, salt solution and simulated concrete pore solution on the properties of composite matrix resins used in civil engineering applications". *Polymer Composites*, 22(2), 282-297.

Davalos, J.F., Chen, Y., and Ray, I. (2012). "Long-term durability prediction models for GFRP bars in concrete environment". *Journal of Composite Materials*, 46(16), 1899-1914.

D'Antino T., Pisani, M.A., and Poggi, C. (2018). "Effect of the environment on the performance of GFRP reinforcing bars". *Composites Part B*, 141, 123-136.

Dejke, V. (2001). "Durability of FRP reinforcement in concrete: Literature review and experiments." Chalmers University, Sweden.

Ferdous, W., Manalo, A., Khennane, A. and Kayali, O. (2015). "Geopolymer concrete-filled pultruded composite beams - Concrete mix design and application". *Cement and Concrete Composites*, 58, 1-13.

Gooranorimi, O and Nanni, A. (2017). "GFRP Reinforcement in Concrete after 15 Years of Service". *ASCE Journal of Composites for Construction*, 21(5), 04017024-1-9.

Kamal A, Boulfiza M. Durability of GFRP rebars in simulated concrete solutions under accelerated aging conditions. ASCE Journal of Composites for Construction 2011; 15(4), 473-481.

Karbhari, V.M., Murphy, K. and Zhang, S. (2002). "Effect of concrete based alkali solutions on short-term durability of E-glass/vinyl ester composites". *Journal of Composite Materials*, 36(17), 2101-2121.

Karbhari, V.M. and Zhang, S. (2003). "E-glass/vinyl ester composites in aqueous environments – I: Experimental results". *Applied Composite Materials*, 10, 19-48.

Karbhari, V.M. and Xian, G. (2009). “Hygrothermal effects of high V_F pultruded unidirectional carbon/epoxy composites: Moisture uptake”. *Composites: Part B*, 40, 41-49.

Kim H, Park Y, You Y. (2008) Short-term durability test for GFRP rods under various environmental conditions. Composites Structures; 83, 37-47.

Manalo A, Benmokrane B, Park K-T, and Lutze D. (2014). Recent developments on FRP bars as internal reinforcement in concrete structures. *Concrete in Australia*, 40, 46-56.

Maranan, G.B., Manalo, A.C., Benmokrane, B., Karunasena, W., and Mendis, P. (2016). “Behavior of concentrically loaded geopolymer-concrete circular columns reinforced longitudinally and transversely with GFRP bars”. *Engineering Structures*, 117, 422-436.

Micelli, F. and Nanni, A. (2004). “Durability of FRP rods for concrete structures”. *Construction and Building Materials*, 18, 491-503.

Mouzakis, D.E., Zoga, H., and Galiotis, C. (2008). “Accelerated environmental ageing of polyester/glass fiber reinforced composites (GFRPCs)”. Composites Part B, 39, 467-475.

Naya, S., Meneses, A., Tarrío-Saavedra, J., Artiaga, R., López-Beceiro, J., and Gracia-Fernández, C. (2013). "New method for estimating shift factors in time–temperature superposition models." *Journal of thermal analysis and calorimetry*, 113(2), 453-460.

Nelson, W. B. (2009). *Accelerated testing: statistical models, test plans, and data analysis*, John Wiley & Sons.

Nkurunziza, G., Debaiky, A., Cousin, P., and Benmokrane, B. (2005). “Durability of GFRP bars: A critical review of literature”. *Progress in Structural Engineering Materials*, 7, 194-209.

Robert M and Benmokrane, B. (2013). “Combined effects of saline solution and moist concrete on long-term durability of GFRP reinforcing bars”. *Construction and Building Materials*, 38, 274-284.

Robert M, Cousin P and Benmokrane, B. (2009). “Durability of GFRP reinforcing bars embedded in moist concrete”. *ASCE Journal of Composites for Construction*, 13, 66-73.

Tannous, F.E. and Saadatmanesh, H. (1999). “Durability of AR glass fiber reinforced plastic bars”. *ASCE Journal of Composites for Construction*, 3(1), 12-19.

Wang, J., GangaRao, H., Liang, R., and Liu, W. (2016). “Durability and prediction models of fiber-reinforced polymer composites under various environmental conditions: A critical review”. *Journal of Reinforced Plastics and Composites*, 35(3), 179–211.

Wang, Z., Zhao, X.L., Xian, G., Wu, G., Singh Raman, R.K., and Al-Saadi, S. (2017). “Durability study on interlaminar shear behaviour of basalt-, glass- and carbon-fibre reinforced polymer (B/G/CFRP) bars in seawater sea sand concrete environment”. *Construction and Building Materials*, 156, 985-1004.